the plant journal

SEB SOCIETY FOR EXPERIMENTAL BIOLOGY

The Plant Journal (2010) **61**, 728–740 doi: 10.1111/j.1365-313X.2009.04103.x

Two functionally distinct members of the MATE (multi-drug and toxic compound extrusion) family of transporters potentially underlie two major aluminum tolerance QTLs in maize

Lyza G. Maron[1], Miguel A. Piñeros[1], Claudia T. Guimarães[2], Jurandir V. Magalhaes[2], Jennifer K. Pleiman[1], Chuanzao Mao[1,3], Jon Shaff[1], Silvia N.J. Belicuas[2] and Leon V. Kochian[1,*]

[1]*Robert W. Holley Center for Agriculture and Health, USDA Agricultural Research Service, Cornell University, Ithaca, NY 14853, USA,*

[2]*EMBRAPA Maize and Sorghum, Rod. MG424, km 65, 35701-970, Sete Lagoas, Minas Gerais, Brazil, and*

[3]*State Key Laboratory of Plant Physiology and Biochemistry, College of LifeSciences, Zhejiang University, Hangzhou 310058, China*

Received 20 August 2009; revised 11 November 2009; accepted 16 November 2009; published online 22 January 2010.
*For correspondence (fax +1 607 255 2459; e-mail Leon.kochian@ars.usda.gov).

SUMMARY

Crop yields are significantly reduced by aluminum (Al) toxicity on acidic soils, which comprise up to 50% of the world's arable land. Al-activated release of ligands (such as organic acids) from the roots is a major Al tolerance mechanism in plants. In maize, Al-activated root citrate exudation plays an important role in tolerance. However, maize Al tolerance is a complex trait involving multiple genes and physiological mechanisms. Recently, transporters from the MATE family have been shown to mediate Al-activated citrate exudation in a number of plant species. Here we describe the cloning and characterization of two MATE family members in maize, *ZmMATE1* and *ZmMATE2*, which co-localize to major Al tolerance QTL. Both genes encode plasma membrane proteins that mediate significant anion efflux when expressed in *Xenopus* oocytes. *ZmMATE1* expression is mostly concentrated in root tissues, is up-regulated by Al and is significantly higher in Al-tolerant maize genotypes. In contrast, *ZmMATE2* expression is not specifically localized to any particular tissue and does not respond to Al. [^{14}C]-citrate efflux experiments in oocytes demonstrate that ZmMATE1 is a citrate transporter. In addition, *ZmMATE1* expression confers a significant increase in Al tolerance in transgenic Arabidopsis. Our data suggests that *ZmMATE1* is a functional homolog of the Al tolerance genes recently characterized in sorghum, barley and Arabidopsis, and is likely to underlie the largest maize Al tolerance QTL found on chromosome 6. However, *ZmMATE2* most likely does not encode a citrate transporter, and could be involved in a novel Al tolerance mechanism.

Keywords: aluminum, tolerance, multi-drug and toxic compound extrusion (MATE), transporter, maize, organic acids.

INTRODUCTION

Most crop species undergo a substantial loss in yield when grown on acidic soils, mainly due to the presence of phytotoxic forms of aluminum (Al^{3+}), which become solubilized at soil pH values at or below 5. Plant species have evolved various mechanisms to overcome this stress, by either preventing Al from entering the root (i.e. Al exclusion) or neutralizing the toxic Al^{3+} absorbed by root cells. Exclusion of Al via exudation of organic acid anions from the roots is currently the best documented and most widespread mechanism of Al tolerance. Organic acid anions such as malate, citrate and oxalate chelate Al^{3+} in the rhizosphere, forming stable, non-toxic complexes. This mechanism has been correlated with differential Al tolerance in a large number of monocot and dicot species (Kochian *et al.*, 2004).

The genetics of Al tolerance have also been the focus of considerable research. In wheat (*Triticum aestivum*),

Al tolerance is controlled by a single major locus (Alt_{BH}) that controls nearly 85% of the phenotypic variation in a mapping population (Riede and Anderson, 1996). Similarly, Al tolerance in sorghum (*Sorghum bicolor*) is controlled by a single locus (Alt_{SB}) that explains nearly 80% of the phenotypic variation (Magalhaes *et al.*, 2004). The molecular basis for these loci has been recently elucidated through cloning of the wheat gene *TaALMT1* and the sorghum gene *SbMATE*. Characterization of these genes has shed new light onto the mechanisms of Al-activated organic acid release and contributed significantly to the growing body of evidence indicating that activation of transport is the main regulatory step in the root organic acid exudation response in a number of plant species.

Wheat *TaALMT1* (for Al-activated Malate Transporter) was the first Al tolerance gene isolated in plants, and it encodes an Al-activated malate transporter that is expressed specifically in the root tips of Al-tolerant wheat genotypes (Sasaki *et al.*, 2004; Raman *et al.*, 2005). *TaALMT1* homologs have been shown to encode malate transporters involved in Al tolerance in Arabidopsis (*Arabidopsis thaliana*) and *Brassica napus* (Hoekenga *et al.*, 2006; Ligaba *et al.*, 2006). In addition, a cluster of *TaALMT1* homologs on chromosome 7R of rye (*Secale cereale*) co-localizes with a locus controlling organic anion efflux and Al tolerance (Collins *et al.*, 2008).

The major Al tolerance gene identified in sorghum is a member of the multi-drug and toxic compound extrusion (MATE) family of transporters (Magalhaes *et al.*, 2007). *SbMATE* encodes a plasma membrane citrate transporter that is responsible for the Al-activated exudation of citrate from sorghum root tips. Evidence for a role for MATE transporters in Al tolerance is rapidly accumulating, with the recent cloning of *HvMATE*, which is responsible for citrate exudation in response to Al stress in barley (*Hordeum vulgare* L.) (Furukawa *et al.*, 2007), and *AtMATE* responsible for the citrate release in Arabidopsis that acts as a secondary Al tolerance mechanism operating in conjunction with AtALMT1-mediated malate exudation (Liu *et al.*, 2009). Evidence for a similar situation in wheat has been recently presented, as it has been shown that root citrate release possibly mediated by a MATE transporter is a second Al tolerance mechanism of lesser effect (Ryan *et al.*, 2009).

In maize (*Zea mays*), Al tolerance is associated with high rates of root citrate exudation (Pellet *et al.*, 1995; Piñeros *et al.*, 2002). However, several genetic studies have described maize Al tolerance as a quantitative trait, subject to additive gene effects (Magnavaca *et al.*, 1987; Pandey *et al.*, 1994; Borrero *et al.*, 1995). A QTL mapping study identified five distinct genomic regions regulating Al tolerance in maize (Ninamango-Cárdenas *et al.*, 2003). Evidence from physiological studies also indicates that, in contrast to other species, Al tolerance in maize is a complex phenomenon involving multiple genes and probably multiple physiological mechanisms.

Piñeros *et al.* (2005) suggested that, although root citrate release plays a crucial role in maize Al tolerance, it is likely that other mechanisms not involving organic acid exudation also operate in maize roots.

In an attempt to elucidate the molecular basis of maize Al tolerance, we recently performed a detailed temporal analysis of root gene expression under Al stress using microarrays with Al-tolerant and Al-sensitive maize genotypes (Maron *et al.*, 2008). A number of oligonucleotides representing MATE genes that showed expression patterns consistent with a potential role in Al tolerance were identified. In the present study, we have used a combination of genetic and functional approaches to identify and characterize, among the genes from the microarray study, two members of the MATE family, *ZmMATE1* and *ZmMATE2*, that represent strong candidates for the genes underlying the two major Al tolerance QTL in maize.

RESULTS

Microarray data on MATE-like genes indicate two specific ORFs in the maize genome

The oligonucleotides on the maize microarray representing MATE-like sequences showing differential expression under Al stress (Maron *et al.*, 2008) were closely examined. As a starting point, the sequence of each 80-mer was searched against the partial maize genome sequence database at the National Center for Biotechnology Information (NCBI) using BlastN. Three oligonucleotides (MZ00013115, MZ00021801 and MZ00025698), which originally represented three distinct ESTs in the microarray, localized to the same region of maize chromosome 6, overlapped by two partially sequenced BACs (c0026J18 and b0353K03). The three oligonucleotides were located within the predicted ORF/3′ UTR of the same MATE-like gene (Figure 1a), and had shown very similar patterns of expression in the microarray (Figure 1b), indicating that they very likely represent the same gene.

Two other oligonucleotides (MZ00015089 and MZ00038934), also originally representing distinct ESTs, displayed constitutively higher expression in root tips of the tolerant genotype and landed on the same region of chromosome 5, on the partially sequenced maize BAC c0325C16. MZ00015089 was located at the coding region (split by an intron), and MZ00038934 was located at the end of the last exon/beginning of the 3′ UTR of a predicted ORF encoding another MATE-like gene (Figure 1c). As in the case of the previous oligonucleotides, these also had shown very similar patterns of expression in the microarray (Figure 1d), indicating that they also probably represent the same gene.

The two MATE genes identified in the microarray co-localize with two major Al tolerance QTL

In order to verify whether these two MATE genes co-localize with Al tolerance QTL, they were mapped in a recombinant

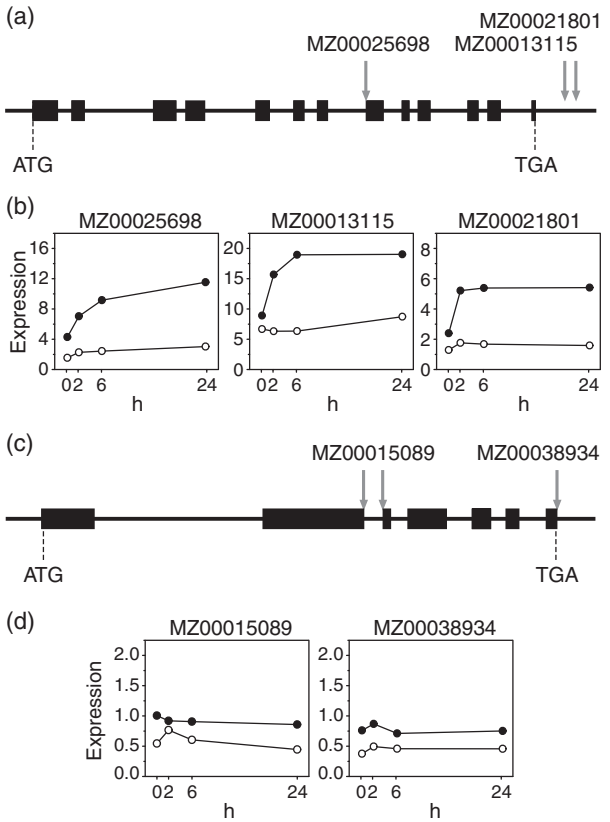

Figure 1. Oligonucleotides in the maize microarray with similar expression patterns target the same genes in the maize genome.
(a, c) Schematic representation of the intron/exon structures of *ZmMATE1* (a) and *ZmMATE2* (c). Exons are represented by black boxes. The location of the microarray oligonucleotides that hybridize to these sequences is indicated by arrows.
(b, d) Expression profiles in response to Al stress for each oligonucleotide hybridizing to *ZmMATE1* and *ZmMATE2*, respectively. Expression levels are represented by their estimated least-square means (see Maron *et al.*, 2008) in genotypes C100-6 (closed circles; Al-tolerant) and L53 (open circles; Al-sensitive).

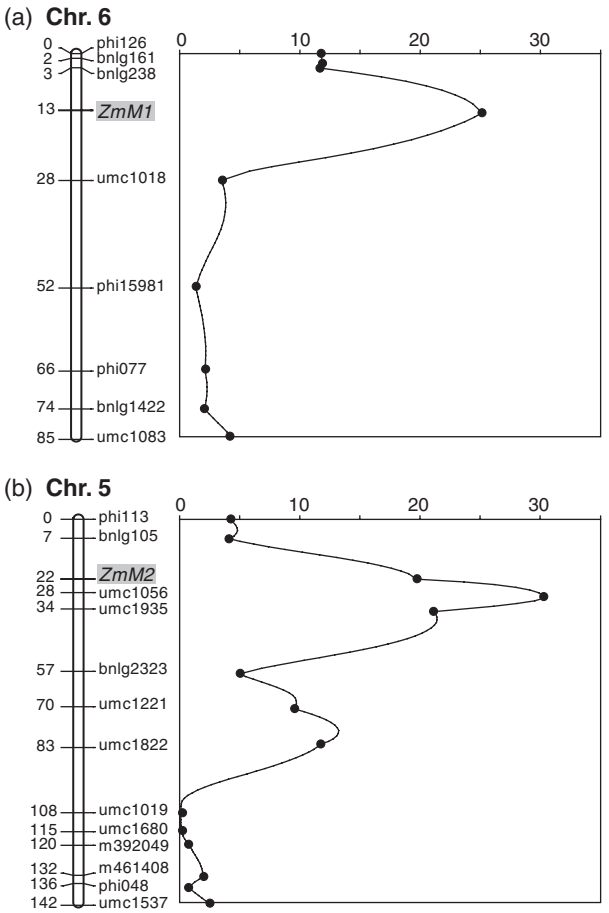

Figure 2. Mapping of (a) *ZmMATE1* and (b) *ZmMATE2*. Two major Al tolerance QTLs located on maize chromosomes 6 (bin 6.00) and 5 (bin 5.03) are shown. Molecular markers were mapped along the linkage groups using genetic distances (cM) calculated by the Kosambi mapping function. Likelihood ratio (LR) peaks indicate the presence of significant QTLs using multiple interval mapping and Bayesian Information Criteria for model selection. The highest LR peaks in chromosomes 6 and 5 are coincident with *ZmMATE1* (*ZmM1*) and *ZmMATE2* (*ZmM2*), respectively.

inbred line (RIL) population generated from the same parental lines used in the maize Al tolerance QTL study described by Ninamango-Cárdenas *et al.* (2003). The first MATE, henceforth referred to as *ZmMATE1*, landed on a telomeric region of maize chromosome 6 (bin 6.00, between the SSR markers bnlg238 and umc1018), co-localizing with an important Al tolerance QTL (Figure 2a). The effect of this QTL, which previously explained 14% of the phenotypic variance (Guimarães, unpublished results), was increased to 16.2% by addition of *ZmMATE1* to the map.

The second MATE (henceforth referred to as *ZmMATE2*) was mapped between markers bnlg105 and umc1056, located at bins 5.02 and 5.03 (Figure 2b) and within the second highest-effect QTL, explaining 16% of the phenotypic variance for Al tolerance in the updated map. Addition of *ZmMATE1* and *ZmMATE2* to the map increased the total phenotypic variance explained from 50% to approximately 66.6%, indicating the importance of these loci to the overall genetic basis of aluminum tolerance in this population.

Cloning of *ZmMATE1* and *ZmMATE2*

The cDNAs of the two MATE genes identified above were cloned from the parental lines of the mapping population [Cateto Al237 (Al-tolerant) and L53 (Al-sensitive)] as well as from C100-6 (Al-tolerant), which was used alongside L53 in the microarray study (Maron *et al.*, 2008). *ZmMATE1* encodes a 563 amino acid protein (Figure 3a,c), and its genomic structure consists of 13 exons (see Figure 1a). The cDNA sequences obtained from Al237 and C100-6 were identical, while the cDNA sequence from L53 showed six nucleotide substitutions within the coding region when compared to Al237/C100-6, resulting in two non-conserved

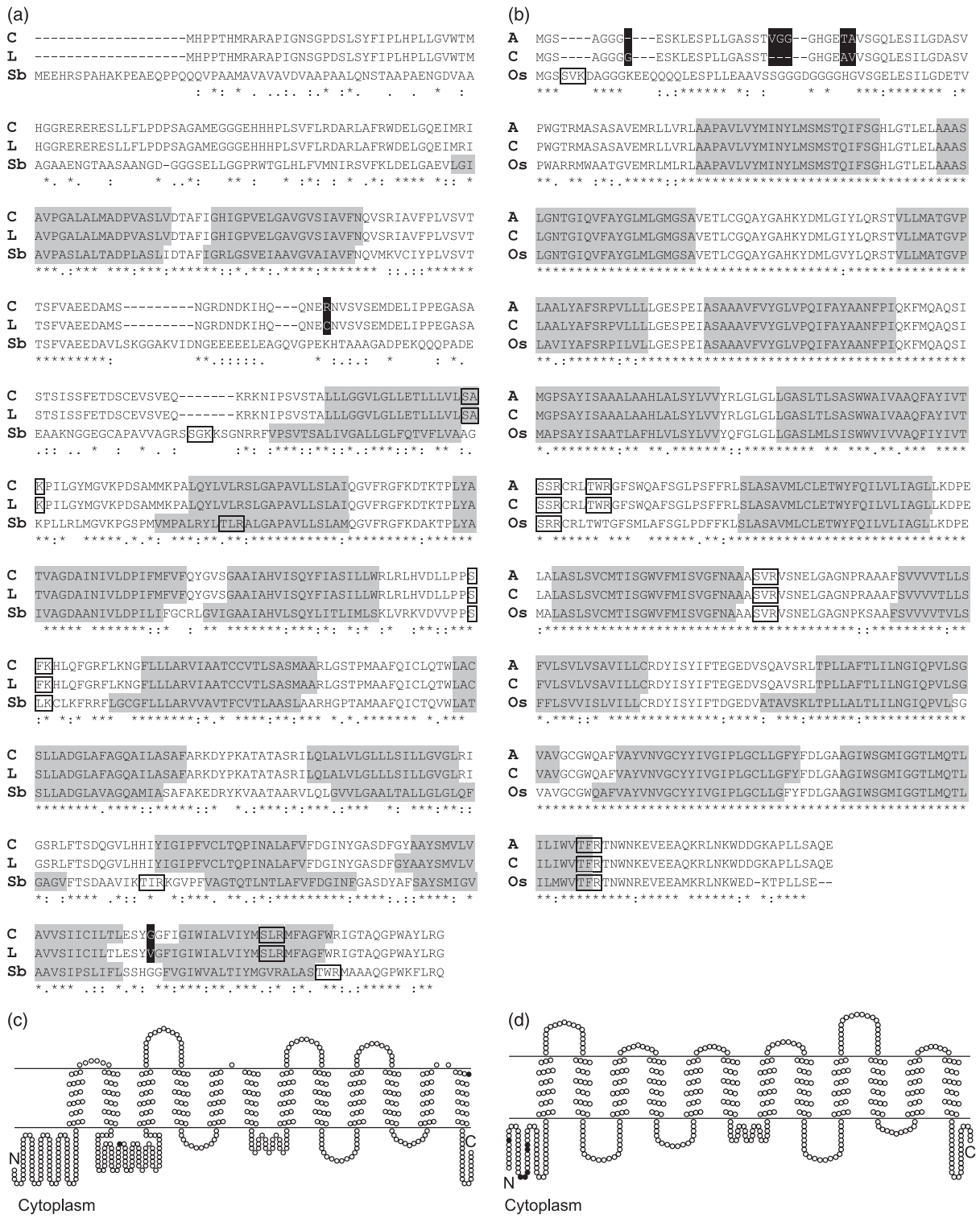

Figure 3. Amino acid sequence and structure predictions for ZmMATE1 and ZmMATE2.
(a) Clustal W alignment of the deduced amino acid sequences of ZmMATE1 (C, C100-6 and Al237 sequences; L, L53 sequence) and SbMATE.
(b) Clustal W alignment of the deduced amino acid sequences of ZmMATE2 (A, Al237 and L53 sequences; C, C100-6 sequence) and of rice Os03g37490. Symbols under the alignments indicate identical (*), strongly conserved (:) or weakly conserved (.) residues according to the BLOSUM62 matrix. Predicted transmembrane domains are shaded gray. Amino acid substitutions between the sequences of the various genotypes are indicated by black boxes. The predicted locations of putative protein kinase C phosphorylation three amino acid motifs, determined using PROSITE (http://www.expasy.ch/prosite), are indicated by open boxes.
(c, d) Structural predictions for ZmMATE1 and ZmMATE2 proteins, respectively, according to ConPred II (Arai *et al.*, 2004). The positions of the amino acid substitutions between the various genotypes are marked in black.

amino acid substitutions at positions 171 and 527 (Figure 3a). The predicted protein sequence shares significant amino acid identity to sorghum SbMATE (52%) and Arabidopsis AtMATE (64%). The predicted secondary structure of ZmMATE1 consists of 12 transmembrane domains (Figure 3a,c), and the position of these domains appears to be conserved between SbMATE and ZmMATE1. In addition, three potential phosphorylation sites for protein kinase C were identified in ZmMATE1, of which one is also found in the same position in SbMATE.

ZmMATE2 encodes a 513 (or 511) amino acid protein (Figure 3b,d), and its genomic structure consists of seven exons (see Figure 1c). The cDNA sequences from genotypes Al237 and L53 showed 12 nucleotide substitutions within the coding region; however, all of them are silent, so that the predicted proteins are identical. The cDNA sequence from C100-6, on the other hand, contained 12 nucleotide substitutions relative to Al237, two of which result in semi-conserved amino acid substitutions at positions 30/31. In addition, a three-nucleotide insertion and a nine-nucleotide deletion were present, causing a one amino acid insertion and a three amino acid deletion at positions 8 and 23/25, respectively (Figure 3b). The resulting ZmMATE2 protein predicted for C100-6 therefore contains 511 amino acids. Unlike ZmMATE1, the predicted ZmMATE2 protein does not share identity with any MATE proteins recently characterized as citrate transporters. Instead, the best match to ZmMATE2 is a rice protein of unknown function, Os03g37490, with which it shares significant amino acid identity (85%). The predicted secondary structure of ZmMATE2 consists of 12 transmembrane domains (Figure 3b,d), which are all also present in Os03g37490. In addition, three potential phosphorylation sites for protein kinase C were identified in ZmMATE2, of which two are present in the same position in Os03g37490.

ZmMATE1 and *ZmMATE2* have unique patterns of expression

Gene expression patterns for *ZmMATE1* and *ZmMATE2* were monitored using quantitative real-time PCR (Figure 4). Over a time course of Al exposure in root tips, *ZmMATE1* expression remained constant under control conditions, but was strongly up-regulated by Al as early as 1 h after exposure in both tolerant genotypes Al237 and C100-6, and to much lesser extent in the Al-sensitive genotype L53 (Figure 4a). Constitutive *ZmMATE1* expression was 5 to 10-fold higher in the Al-tolerant genotypes than in the Al-sensitive one. In addition, *ZmMATE1* expression was evaluated in various parts of the plant (Figure 4b). *ZmMATE1* transcript accumulation was concentrated in the root tip (1 cm), and was also detected at a lower level in the rest of the root. Up-regulation of gene expression by Al treatment was primarily localized to the root tissues, particularly root tips.

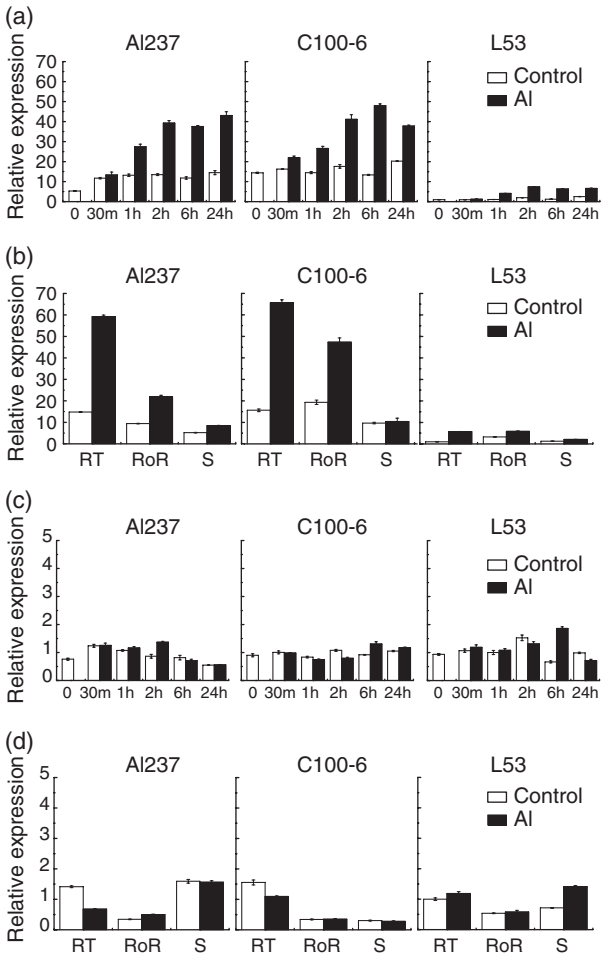

Figure 4. Temporal and spatial gene expression profiles for *ZmMATE1* (a, b) and *ZmMATE2* (c, d).
Quantitative real-time PCR was performed using total RNA collected from maize seedlings.
(a, c) Time courses of (a) *ZmMATE1* and (c) *ZmMATE2* expression in root tips treated with 0 (control) or 39 μM Al^{3+} activity (Al) for 0, 30 min, or 1, 2, 6 or 24 h.
(b, d) Spatial profiles of (b) *ZmMATE1* and (d) *ZmMATE2* expression in root tips (RT), rest of the root (RoR) and shoots (S) of plants treated with 0 (control) or 39 μM Al^{3+} activity (Al) for 24 h.

ZmMATE2 displayed a strikingly different expression pattern. In a time course study in root tips, the levels of *ZmMATE2* transcript remained nearly constant in all three genotypes and did not seem to respond to Al (Figure 4c). Only a small, transient up-regulation of *ZmMATE2* expression was observed after 6 h of Al exposure in Al-sensitive L53 root tips. *ZmMATE2* expression throughout the plant also followed a different pattern from that of *ZmMATE1* (Figure 4d). Unlike *ZmMATE1*, *ZmMATE2* expression did not appear to be concentrated in the root. In genotypes Al237 and L53, the levels of *ZmMATE2* transcript in root tips and shoots were similar, but were slightly lower in

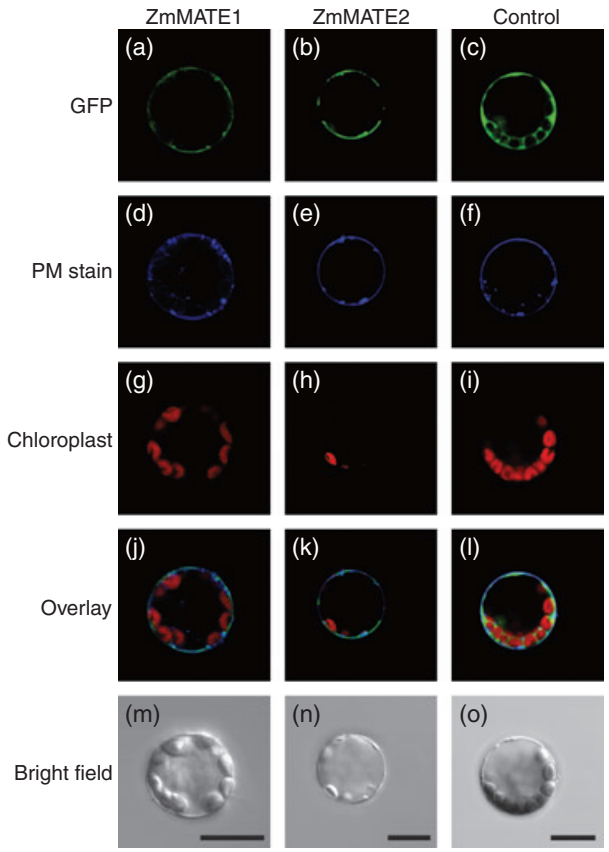

Figure 5. Cellular localization of ZmMATE1 and ZmMATE2 proteins in Arabidopsis protoplasts.
The first, second and third columns show representatives cells transformed with ZmMATE1::GFP; ZmMATE2::GFP and pSAT6A empty vector as a control. The first row (a–c) shows GFP fluorescence patterns; the second row (d–f) shows CellMask plasma membrane stain fluorescence patterns; the third row (g–i) shows chloroplast autofluorescence; the fourth row (j–l) shows an overlay of the fluorescent images; the fifth row (m–o) shows a bright-field image of each protoplast. Images are representative of four independent experiments in which ≥20 protoplasts were imaged. Scale bar = 15 μm.

the rest of the root. In C100-6, *ZmMATE2* expression levels in the root tips were comparable to those in the other two genotypes; however, expression was lower in C100-6 shoots.

ZmMATE1::GFP and *ZmMATE2*::GFP localize to the plasma membrane of plant cells

The cellular localization of ZmMATE1 and ZmMATE2 proteins was investigated using transient expression assays of translational fusions with green fluorescent protein (GFP) in Arabidopsis leaf protoplasts (Figure 5). In protoplasts transformed with *ZmMATE1*::GFP (Figure 5a) and *ZmMATE2*::GFP (Figure 5b), green fluorescence was localized to the cell periphery, suggesting a plasma membrane localization. In contrast, in control protoplasts (transformed with the empty vector), green fluorescence was observed in the cytosol (Figure 5c). In order to confirm the localization of the ZmMATE1 and ZmMATE2 proteins to the plasma membrane, protoplasts were stained with a fluorescent dye that specifically labels the plasma membrane (Figure 5d–f). In protoplasts transformed with *ZmMATE1*::GFP (Figure 5d) and *ZmMATE2*::GFP (Figure 5e), GFP fluorescence co-localized with fluorescence from the plasma membrane dye, while the GFP fluorescence in control protoplasts was seen in the cytoplasm, inside the stained plasma membrane (see overlay images in Figure 5j–l). These results indicate that both ZmMATE1 and ZmMATE2 proteins localize to the plasma membrane.

ZmMATE1 and ZmMATE2 mediate anion transport in *Xenopus* oocytes

Functional characterization of the transport properties of ZmMATE1 and ZmMATE2 was performed by examining the electrophysiological characteristics of *Xenopus* oocytes expressing these proteins. Oocytes injected with either ZmMATE1 or ZmMATE2 cRNA had significantly less negative resting membrane potentials (RMP) than control cells (Figure 6a). Pre-loading ZmMATE1- and ZmMATE2-expressing cells with sodium citrate resulted in membrane potential polarization, with cells showing more negative RMPs relative to unloaded cells. These results indicate that expression of either ZmMATE causes a reduction in the internal negative charge (relative to that of control cells) as a result of an increase in net anion efflux or net cation influx. Further characterization was performed using the two-electrode voltage clamp technique (TEVC). ZmMATE1-expressing cells showed large, slowly activating inward currents that were significantly larger than those elicited in control cells using identical voltage protocols (Figure 6b,c). By convention, inward currents are the product of net positive charge influx (e.g. Na^+ or H^+) or net negative charge efflux (e.g. organic or inorganic anions). Decreasing the pH of the bath medium resulted in a significant increase in the magnitude of ZmMATE1-mediated inward currents, suggesting that ZmMATE1 mediates proton-coupled transport. In contrast, addition of Al^{3+} to the bathing solution significantly decreased the magnitude of ZmMATE1-mediated inward currents (Figure 6c, inset). In comparison, under these various ionic conditions, cells expressing ZmMATE2 did not show any significant change in inward currents relative to control cells.

Further characterization of ZmMATE-mediated transport was performed by removing NaCl from the bath solution, thus minimizing the extracellular cation concentration and cation influx driving force (Figure 7a–c). Under these conditions, ZmMATE1 still mediated significantly larger negative currents relative to control cells, while ZmMATE2-expressing cells displayed significant inward current activity, with the magnitude of the ZmMATE2-mediated currents being smaller than those due to ZmMATE1. The change in the

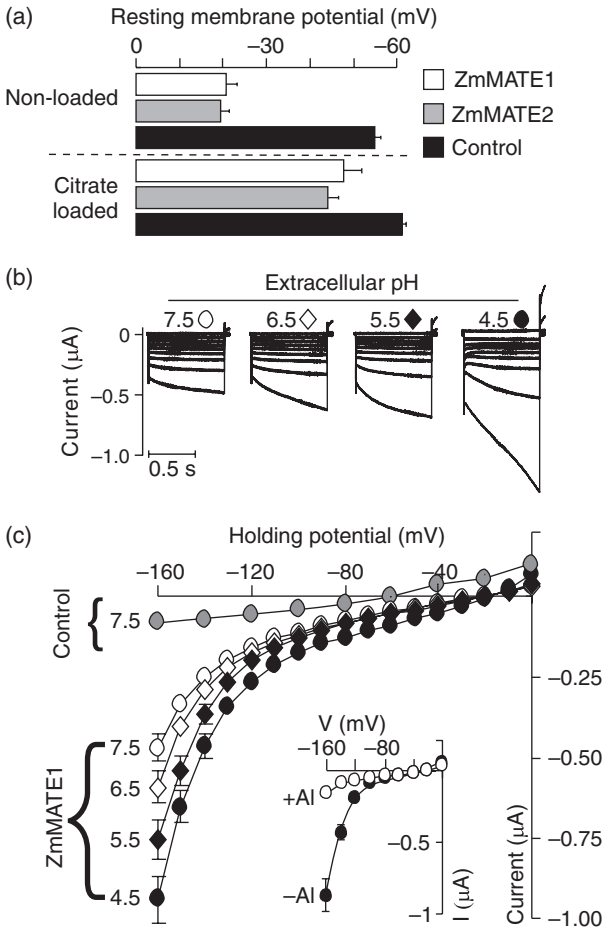

Figure 6. Functional characteristics of ZmMATE1 and ZmMATE2 expressed in *Xenopus* oocytes.
(a) Resting membrane potentials (RMP) of control, ZmMATE1- and ZmMATE2-expressing cells measured in ND96 (pH 7.5). RMPs are shown for unloaded cells and cells pre-loaded with citrate. Pre-loading was performed 2 h prior to recording by injecting 48 nl of 0.1 M sodium citrate (pH 7.2), resulting in a theoretical intracellular concentration of approximately 9 mM sodium citrate (assuming a cell diameter of 1 mm) (n = 12 cells).
(b) Examples of families of currents from ZmMATE1-expressing cells recorded in ND96 solution at various pH values in response to voltage pulses ranging from −160 to 0 mV in 20 mV steps.
(c) Mean current/voltage (I/V) relationship from the recordings shown in (b). The symbols correspond to those indicated in (b). Current magnitudes from control cells (oocytes not injected with cRNA; gray circles) bathed in ND96, pH 7.5, are shown for reference. The inset illustrates the inhibition of ZmMATE1 currents upon addition of 100 μM $AlCl_3$ to the ND96 bath solution, pH 4.5.

reversal potential (E_{rev}, the holding potential at which the current changes sign) for the current-to-voltage relationships upon lowering NaCl is consistent with anion transport dictating the positive shift in E_{rev}. Addition of exogenous citrate or malate to the medium resulted in an increase in the inward currents mediated by both ZmMATEs, with the increase being significantly larger in ZmMATE1-expressing cells. Removal of organic acids from the medium resulted in the currents returning to original resting levels. Likewise, the increase in magnitude of the inward current was dependent on the concentration of citrate supplied in the bath medium. In contrast, the small inward current recorded in control cells was not altered by the presence of either citrate or malate in the bath solution. These results substantiate the anion-permeable nature of ZmMATE1- and ZmMATE2-mediated transport. To further elucidate the identity of the ZmMATE-mediated proton-coupled anion transport, we studied citrate efflux from oocytes expressing ZmMATE1 and ZmMATE2 by measuring the efflux of radioactively labeled citrate from cells loaded with [^{14}C]-citrate. ^{14}C efflux from cells expressing ZmMATE1 was at least twice that observed in control cells (Figure 7d). These results indicate that ZmMATE1 can mediate citrate efflux, and further confirm that anion efflux underlies the ZmMATE1-mediated transport recorded in TEVC experiments. In contrast, ZmMATE2-expressing cells did not show any significant ^{14}C efflux relative to that observed in control cells, suggesting that, at least under these ionic conditions, ZmMATE2 does not transport citrate, in agreement with the lack of significant inward currents observed in TEVC experiments under the same set of ionic conditions.

ZmMATE1 expression in transgenic Arabidopsis confers an increase in Al tolerance

The coding region of *ZmMATE1* was stably introduced into Arabidopsis plants (ecotype Columbia), driven by the CaMV 35S promoter. Homozygous T_3 lines were selected and studied in terms of root growth and root citrate exudation under Al stress (Figure 8). When grown in agar medium in the absence of Al, transgenic plants expressing *ZmMATE1* (as well as plants carrying the empty vector as a control) exhibited root growth similar to that of wild-type Columbia plants (Figure 8a). On the other hand, when grown in agar medium in the presence of Al, transgenic plants expressing *ZmMATE1* exhibited almost no root growth inhibition, in contrast with ecotype Columbia plants, which exhibited significant root growth inhibition. In addition, transgenic plants carrying the empty vector performed similarly to wild-type plants.

Root citrate exudation was also analyzed in the T_3 homozygous lines showing increased Al tolerance (Figure 8b). Transgenic plants expressing *ZmMATE1* exhibited a significant increase in the rates of root citrate exudation when compared to wild-type, both in the presence and in the absence of Al. In contrast, transgenic plants carrying the empty vector showed citrate exudation rates similar to those of wild-type plants.

DISCUSSION

The maize genome is not yet fully sequenced, and is known for its complexity, the presence of repetitive elements and an extensive degree of polymorphism and duplication. Therefore, positional cloning of QTL in maize is often a

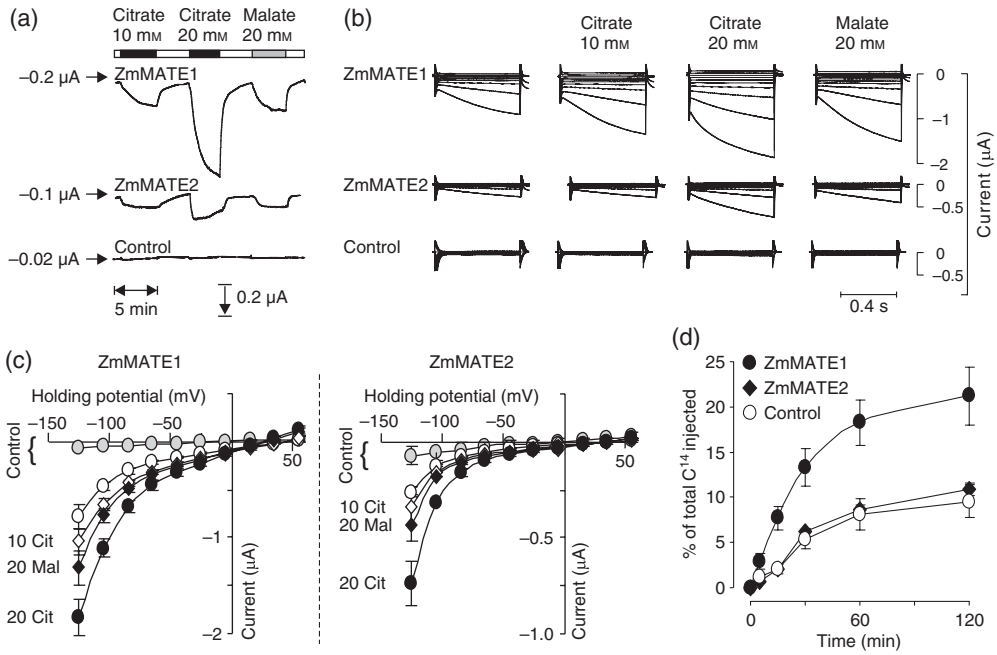

Figure 7. ZmMATE1 and ZmMATE2 mediate anion transport.
(a) Representative traces illustrating the increase in inward (i.e. negative) ZmMATE1- and ZmMATE2-mediated currents elicited upon exposure to extracellular citrate or malate. The presence and concentration of citrate or malate is indicated by black and gray bars (respectively) above the current trace. The ionic composition of the solution was 1 mM $MgCl_2$ and 1.8 mM $CaCl_2$ (pH 4.5 and 200 mosmol kg^{-1} adjusted with 5 mM MES/Tris and D-sorbitol, respectively). The membrane potential was clamped at –60 mV. The arrows on the left of each trace indicate current magnitude prior to the addition of citrate or malate. Time and current scales are indicated below the trace from the control cell.
(b) Examples of families of currents from ZmMATE1- and ZmMATE2-expressing cells in response to voltage pulses ranging from –140 to +40 mV in 20 mV steps recorded under the ionic conditions described in (a).
(c) Mean current/voltage (*I/V*) relationship from the recordings as shown in (b). Current magnitudes from control cells (oocytes not injected with cRNA; gray circles) bathed in the absence of citrate or malate are shown for reference. Note the difference in the current (*y* axis) scale between the *I/V* curves.
(d) [^{14}C]-citrate efflux in oocytes. Control, ZmMATE1- and ZmMATE2-expressing oocytes injected with [^{14}C]-citrate were kept in ND96 solution (pH 4.5). The radioactivity in the bathing solution was measured at the indicated time points; values are expressed as a percentage of the total radioactivity injected.

challenging and time-consuming approach (Bortiri *et al.*, 2006). In this study, the combination of genetic mapping with gene expression data allowed us to identify and characterize candidates for the genes underlying the two major Al tolerance QTL in a maize mapping population, *ZmMATE1* and *ZmMATE2*. Al tolerance QTL in the genomic region of *ZmMATE1* have been independently identified in various mapping populations by Sibov *et al.* (1999), using C100-6 as the Al-tolerant parental line, by Ninamango- Cárdenas *et al.* (2003), and in the current RIL population. In the genomic region spanning *ZmMATE2*, Ninamango- Cárdenas *et al.* (2003) reported an RFLP marker (umc043) that explains 10.6% of the phenotypic variance. In the current RIL population, *ZmMATE1* and *ZmMATE2* map to the two major Al tolerance QTL, and their combined effects explain a large proportion of the total phenotypic variance in Al tolerance.

MATE proteins are widely distributed in all kingdoms of living organisms; however, their functions are still largely unknown (Omote *et al.*, 2006). In bacteria, the few MATE transporters that have been characterized export cationic drugs through H^+ or Na^+ exchange. There is no apparent consensus sequence shared among all MATE proteins, although these proteins exhibit around 40% sequence similarity (Moriyama *et al.*, 2008). In contrast to the presence of few MATE genes per species in bacteria and animals, plant MATE transporters have many orthologs and only a few have been functionally characterized. Plant MATE proteins capable of transporting citrate have recently been identified; some of these act as the transporter responsible for Al-activated root citrate release underlying Al tolerance (Furukawa *et al.*, 2007; Magalhaes *et al.*, 2007; Liu *et al.*, 2009), while others are citrate transporters related to other physiological processes such as iron translocation (Durrett *et al.*, 2007; Yokosho *et al.*, 2009) and phosphorus efficiency (Uhde-Stone *et al.*, 2003). In addition, plant MATE proteins with specificity for a variety of substrates such as flavonoids (Debeaujon *et al.*, 2001), xenobiotics (Li *et al.*, 2002; Otani *et al.*, 2005) and alkaloids (Morita *et al.*, 2009) have been identified. The presence of a large number of genes encoding MATE proteins that transport a variety of substrates suggests that transporters of this family must perform an array of biological roles in plants.

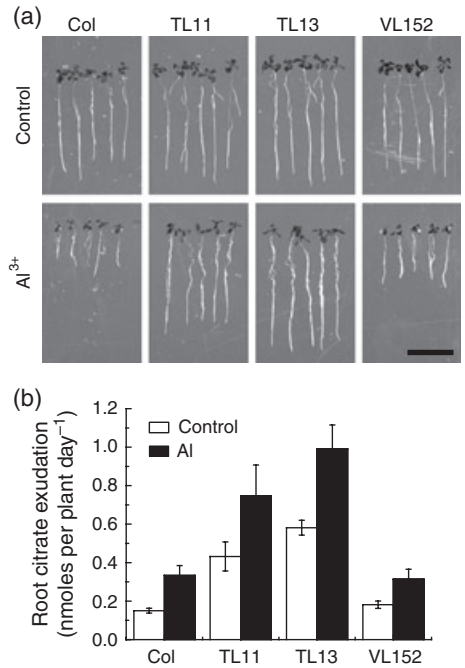

Figure 8. Expression of *ZmMATE1* in transgenic Arabidopsis plants.
(a) Al tolerance of T_3 homozygous lines expressing *ZmMATE1* under the control of the 35S promoter. Root growth of representative plants from two independent transgenic lines grown in agar medium in the absence (top row) or presence (bottom row) of Al^{3+} for 14 days. Scale bar = 1 cm.
(b) Root citrate exudation in the absence or presence of Al^{3+} of T_3 homozygous lines expressing *ZmMATE1* under the control of the 35S promoter. Data collected are from four replicas comprising an average of 180 plants each. Col, wild-type Columbia; TL11 and TL13, transgenic lines expressing *ZmMATE1*; VL152, transgenic line carrying only empty vector as a control.

ZmMATE1

The evidence presented in this report strongly suggests that *ZmMATE1* is a functional homolog of the sorghum Al tolerance gene *SbMATE*. ZmMATE1 has significant amino acid identity to SbMATE as well as a conserved transmembrane domain structure (Figure 3). Similarly to *SbMATE*, expression of *ZmMATE1* in transgenic Arabidopsis plants confers a significant increase in Al tolerance and root citrate exudation (Figure 8). *ZmMATE1* expression is concentrated in the root tissues and is considerably higher in Al-tolerant genotypes (Figure 4). The small (two amino acid) differences in the ZmMATE1 proteins encoded by the various genotypes are unlikely to cause dramatic changes to the functionality of the protein, and it appears that the levels of *ZmMATE1* expression are correlated with the degree of Al tolerance observed in various genotypes. Levels of *ZmMATE1* expression are not only constitutively higher in the Al-tolerant genotypes when compared to the sensitive genotype, but are also much more strongly up-regulated by Al. It is also interesting to note that the timing of *ZmMATE1* up-regulation by Al is closely correlated with the onset of Al-activated root citrate release; increased *ZmMATE1* expression in root tips can be detected as early as after 1 h of Al exposure (Figure 4a), while citrate release from roots of the Al-tolerant C100-6 can be detected after 2 h of Al exposure (see Maron *et al.*, 2008). The rapid regulation of *ZmMATE1* expression and citrate exudation by Al differs remarkably from what is observed in sorghum. *SbMATE* expression is constitutively high in Al-tolerant genotypes and barely detectable in Al-sensitive genotypes. Al exposure causes only a moderate increase in expression (twofold) (Magalhaes *et al.*, 2007). Interestingly, the activation of citrate exudation in sorghum roots also happens gradually, over the course of 6 days of exposure to Al. These differences suggest that the citrate exudation response in these two plants species is regulated by somewhat different mechanisms. Nevertheless, as expression of the gene encoding the citrate transporter (i.e. *SbMATE* and *ZmMATE1*) is up-regulated upon Al exposure in both species, it is likely that other unknown elements, such as transcription factors, are involved in the response. In addition, citrate exudation is likely to be regulated at the protein level in both maize and sorghum, as *ZmMATE1* and *SbMATE* expression is constitutively high in roots of Al-tolerant genotypes, however, citrate exudation is only activated upon exposure to Al. With this in mind, it is interesting to note that, in transgenic Arabidopsis plants expressing *ZmMATE1* under the control of a constitutive promoter, root citrate release is not only constitutively higher than in wild-type, but is also further increased under Al exposure. This result suggests that at least part of the machinery required for the activation of *ZmMATE1* by Al is present in Arabidopsis. This is not surprising, given that Arabidopsis also uses citrate release as a secondary Al tolerance mechanism, and *AtMATE1* has been shown to be a close homolog of *SbMATE* (Liu *et al.*, 2009).

The functional analysis of *Xenopus* oocytes expressing *ZmMATE1* established that this transporter mediates anion efflux, and is specifically able to mediate citrate efflux (Figures 6 and 7). As mentioned above, bacterial MATE transporters have been described as functioning as sodium or proton antiporters, such that inwardly directed cation gradients energize the efflux of toxins from the cells. Our results indicate that ZmMATE1-mediated efflux was not affected by altering the extracellular Na^+ status, but was rather highly dependent on external pH, suggesting that, in plant cells, MATE transporters, or at least ZmMATE1, mediates anion efflux coupled with proton influx. This situation is intriguing, given that the large negative plasma membrane electrical potential found in plant cells satisfies the thermodynamic requirements for passive efflux of citrate, while proton-coupled antiport is usually associated with the active efflux of solutes.

Organic anion efflux in response to Al stress has been shown to be mediated by ALMT-type transporters in several plant species. The transport and regulatory properties of this

channel-type family of transporters differs significantly from those of MATE transporters, as ALMTs mediate the passive efflux of malate and are directly regulated by extracellular Al^{3+} (Piñeros *et al.*, 2008). In contrast, extracellular Al^{3+} does not directly regulate ZmMATE1 activity, but rather has an inhibitory effect on ZmMATE1-mediated transport (at least in oocytes), suggesting that its regulation and activation upon perception of Al stress *in planta* are achieved via additional elements (e.g. protein–protein interaction, regulatory factors, etc.) present in the signal transduction cascade.

The complexity of the regulation of the Al-activated citrate exudation response and the possible presence of additional Al tolerance mechanisms in maize are in agreement with genetic evidence showing the involvement of multiple genomic regions in controlling this trait.

ZmMATE2

ZmMATE2 is a member of the MATE family and co-localizes with the second largest Al tolerance QTL, making it another interesting candidate Al tolerance gene in maize. Characterization of *ZmMATE2* showed that this gene differs from *ZmMATE1* and from other MATEs involved in Al tolerance in a number of aspects. ZmMATE2 does not share significant amino acid sequence identity with MATEs shown to transport citrate. The pattern of expression of *ZmMATE2* is also quite different from that of *ZmMATE1*. *ZmMATE2* expression is not significantly higher in the Al-tolerant genotypes or up-regulated by Al (Figure 4c). In addition, the ZmMATE2 amino acid sequences encoded by the parents of the RIL mapping population (Cateto Al237 and L53) are identical. This is intriguing as it appears that *ZmMATE2* is not significantly polymorphic between the parents in terms of either expression levels or protein functionality. However, this does not necessarily mean that *ZmMATE2* is less likely to underlie the Al tolerance QTL on maize chromosome 5 where it is localized. This QTL explains approximately 16% of the phenotypic variation for Al tolerance in the RIL population. Therefore, there is a substantial amount of the phenotypic variation (51%) left to other QTL, in addition to the 33% left unexplained by the QTL identified so far. Considering the extremely contrasting degree of Al tolerance displayed by the parents, a possible scenario is that *ZmMATE2* regulation by Al is silent in Al237 (the Al-tolerant parent), which nevertheless retains superior Al tolerance due to the fixation of positive alleles at other QTL. In this case, *ZmMATE2* expression would be triggered by regulatory factor(s) with negative alleles in Al237 but positive alleles in L53 (the Al-sensitive parent). The segregating progeny would include recombinant individuals with positive and negative alleles at each loci, thus resulting in greater phenotypic distribution (i.e. transgressive segregation) for *ZmMATE2* expression in the RILs than in the parents. Extensive transgressive segregation for transcript levels has been observed in yeast (Brem *et al.*, 2002) and more recently in Arabidopsis (West *et al.*, 2007). Particularly in Arabidopsis, it was observed that while the parental microarray data showed significant differences for only 14% of the transcripts, the RIL microarray data detected eQTL for 69% of the e-traits. In other words, the variation of transcript levels in the parents is not predictive of the variation observed in the progeny. Instances of complex regulatory cascades have in fact been found in relation to Al tolerance. In Arabidopsis, the transcription factor STOP1 regulates the expression of both *AtALMT1* and *AtMATE1*, which underlie independent mechanisms of Al tolerance (Liu *et al.*, 2009). Furthermore, STOP1 also regulates the expression of other genes that protect Arabidopsis from Al and pH toxicities (Sawaki *et al.*, 2009). In summary, it is plausible to conjecture that *ZmMATE2* expression is differentially regulated in the RIL population even though this was not observed in the parents, and, as such, could potentially be responsible for the Al tolerance QTL with which it co-localizes on maize chromosome 5.

Piñeros *et al.* (2005) demonstrated that, although correlated with Al-activated root citrate release, Al tolerance in maize cannot be solely explained by this mechanism. Consequently it is reasonable to expect that certain Al tolerance QTLs, particularly those with a secondary effect, control traits that provide Al tolerance independently from root citrate release. The functional analysis of ZmMATE2 in *Xenopus* oocytes showed that ZmMATE2 is capable of mediating significant inward current activity in TEVC experiments when the extracellular cation concentration is minimized, suggesting that it can mediate anion efflux (Figure 7). However, our results also suggest that, unlike ZmMATE1, ZmMATE2 may not mediate citrate efflux, at least not under the ionic conditions tested (Figure 7d). The nature of the substrate transported by ZmMATE2 remains unknown. Therefore, it is possible that ZmMATE2 could be involved in a different Al tolerance mechanism. To date, no Al tolerance mechanisms other than root citrate exudation have been identified in maize. Maize roots also release significant amounts of phosphate and malate, which can chelate Al; however, the exudation rates do not seem to respond to Al exposure (Piñeros *et al.*, 2002). It has also been suggested that Al activates the release of flavonoid-type phenolic compounds from maize roots, and phenolics can be effective chelators of Al^{3+} (Kidd *et al.*, 2001; Barcelo and Poschenrieder, 2002). Interestingly, plant MATE proteins have been identified that transport flavonoids (Debeaujon *et al.*, 2001); nevertheless, the role of phenolic compound exudation in Al tolerance has not yet been firmly established. Recently, Huang *et al.* (2009) identified the first Al tolerance gene in rice, encoding an ATP-binding cassette (ABC) transporter. The protein appears to specifically transport UDP-glucose, which may be involved in rice Al tolerance by altering cell-wall properties. A more in-depth

characterization of the transport properties of ZmMATE2 will be required in order to define what compound(s) it transports. In addition, further genetic and functional characterization will be required to determine whether (and how) this transporter could be related to maize Al tolerance.

EXPERIMENTAL PROCEDURES

Plant growth and Al treatment

Maize seeds were germinated and seedlings were grown in full nutrient solution at pH 4.0 as previously described (Magnavaca *et al.*, 1987; Piñeros *et al.*, 2002). Plants were grown in a growth chamber at 26/24°C (light/dark, 16/8 h). Plants were allowed to acclimatize to the nutrient solution for 24 h prior to time course experiments; the acclimatization period was extended to 48 h when RNA was collected from various parts of the plant so that there was enough shoot tissue available for collection. Aluminum treatment was initiated by replacing the nutrient solution with the same solution containing the amount of aluminum indicated in the text, supplied as $KAl(SO_4)_2$. Free Al^{3+} activities were calculated using GEOCHEM-PC speciation software (Parker *et al.*, 1995).

Mapping of *ZmMATE1* and *ZmMATE2*

The mapping population consisted of 118 RILs derived from a cross between Cateto Al237 (Al-tolerant) and L53 (Al-sensitive). Genomic regions around the oligonucleotides representing *ZmMATE1* and *ZmMATE2* were sequenced from the parental lines to identify polymorphisms to be mapped. For *ZmMATE1*, a 129 bp indel identified in alignments between the parental line sequences was amplified using forward primer 5′-CCGGATGTTTGCTGGATTTT-3′ and reverse primer 5′-TGGCCAAATCGACCATGATT-3′, and resolved in 1% agarose gels stained with ethidium bromide. *ZmMATE2* was mapped using a 10 bp indel with forward primer 5′-GCAGTTCGTACGTAGTGGTG-3′ and reverse primer 5′-AGTACGTAGCTAGGCGATGC-3′ fluorescently labeled, and genotyped using a ABI3100 genetic analyzer (Applied Biosystems, http://www.appliedbiosystems.com/). The complete genetic map consisted of 154 molecular markers including SSRs, STSs and RFLPs, covering 1521.5 cM (Guimaraes, unpublished results). The phenotypic index used for Al tolerance was relative root growth, measured as root growth in nutrient solution containing 39 μM Al^{3+} activity divided by root growth in control solution (no Al). Root growth was defined as final minus initial root length measured after 5 days. The experiment was carried out using a complete randomized design with two replicates, and each plot contained seven plants. QTL mapping was performed using multiple interval mapping (Kao *et al.*, 1999) with the criteria of model selection of Bayesian Information using QTL Cartographer 2.5 (http://statgen.ncsu.edu/qtlcart/WQTLCart.htm).

Cloning of *ZmMATE1* and *ZmMATE2*

The coding region of *ZmMATE1* (genomic and cDNA) was cloned using a combination of 3′/5′ RACE and genome walking strategies. 3′ and 5′ RACE were performed using the SMART RACE cDNA amplification kit (Clontech, http://www.clontech.com). Primers for 3′ and 5′ RACE were designed in the region of the microarray oligonucleotides, and used to obtain partial cDNA clones. Novel sequences obtained were used as templates for new primers for 5′ RACE and genomic walking, performed using the GenomeWalker universal kit (Clontech). After obtaining complete sequences, primers were designed to clone the full-length coding regions in all three genotypes. PCR products were cloned and fully sequenced (GenBank accession numbers FJ015155–FJ015157).

BAC sequences containing the complete ORF of *ZmMATE2* were already available at the time of cloning. The coding region of *ZmMATE2* was cloned directly using primers designed based on the available BAC sequences. PCR products were TA-cloned and fully sequenced (GenBank accession numbers FJ873684–FJ873686).

RNA isolation and quantitative real-time PCR

Total RNA was isolated using the RNeasy plant mini kit (Qiagen; http://www.qiagen.com) according to the manufacturer's instructions. First-strand cDNA was synthesized using the high-capacity cDNA reverse transcription kit (Applied Biosystems, http://www.appliedbiosystems.com) according to the manufacturer's instructions. Quantitative real-time PCR was performed using an ABI 7900HT sequence detection system, 20× custom Taqman assays and 2× Gene Expression Mastermix (Applied Biosystems). Forward primer 5′-TGTGAGTTTGGCGGATGTGT-3′, reverse primer 5′-TCACAATCTAGGCCAGTACAACAGA-3′ and probe 5′-CACTCACATCGTTAAAC-3′ were used for the Taqman assay for *ZmMATE1*. Forward primer 5′-CCTGAGCGAGCGAGCT-3′, reverse primer 5′-CCATCGTGCGTGTATATATATTACGTGTA-3′ and probe 5′-CCGCCGCGTGTATAT-3′ were used for the Taqman assay for *ZmMATE2*. The pre-designed Taqman assay for eukaryotic 18S (Applied Biosystems) was used as endogenous control. Data were analyzed using RQ Manager (version 1.2, Applied Biosystems). Relative expression levels were calculated using the $\Delta\Delta C_T$ method.

Cellular localization of ZmMATE1 and ZmMATE2 proteins

Subcellular localization was determined via transient expression of translational fusions with GFP in Arabidopsis leaf protoplasts. The coding regions (cDNA) of *ZmMATE1* and *ZmMATE2* were subcloned into the expression vector pSAT6A-eGFP-N1 (Tzfira *et al.*, 2005). Transient expression of the ZmMATE1::GFP and ZmMATE2::GFP translational fusions was performed as described by Yoo *et al.* (2007). In brief, Arabidopsis protoplasts were isolated from leaves of 3–4-week-old plants. Leaf strips were digested in a buffer containing cellulose R-10 and macerozyme R-10 (Yakult Pharmaceutical, http://www.yakult.co.jp). Protoplasts were transformed with 20 μg of plasmid DNA via polyethylene glycol transformation and incubated in the dark at room temperature for 10–13 h. The plasma membrane of protoplasts was stained using CellMask Orange (Invitrogen, http://www.invitrogen.com) at a concentration of 2.5 μg/ml for 15 min at 30°C. Imaging of fluorescent proteins in protoplasts was performed using a Leica TCS SP5 laser scanning confocal microscope (http://www.leica-microsystems.com). The excitation/emission filter wavelengths for each channel were as follows: GFP, 488/500–525 nm; CellMask plasma membrane dye, 561/570–586 nm; chloroplast autofluorescence, 561/669–694 nm.

In vitro transcription and cRNA injection

The coding regions (cDNA) of *ZmMATE1* and *ZmMATE2* were cloned into the multiple cloning site of a T7TS vector, which is flanked by the 5′ and 3′ UTRs of the *Xenopus* β-globin gene. cRNA was synthesized from 1 μg of linearized plasmid DNA template using an mMessage mMachine *in vitro* transcription kit (Ambion, http://www.ambion.com) according to the manufacturer's recommendations. Harvesting of stage V–VI *Xenopus laevis* oocytes and cRNA microinjections were performed as described previously (Goldin, 1992; Piñeros *et al.*, 2008). In brief, injected oocytes were incubated in ND88 at 18°C for 2 days prior to electrophysiological and [^{14}C]-citrate efflux measurements.

Electrophysiological measurements

Electrophysiological measurements were performed under two-electrode voltage clamp (TEVC) using a GeneClamp 500 amplifier (Axon Instruments, http://www.axon.com) as described by Piñeros *et al.* (2008). The ND96 bath solution contained 96mM NaCl, 1 mM KCl and 1.8 mM $CaCl_2$. Currents were elicited by voltage pulses stepped between values indicated in the figures, with a 30 sec rest at 0 mV between each pulse. Steady-state current–voltage (*I*/*V*) relationships were generated by measuring the current amplitude at 400 msec after initiation of the test pulse. Liquid junction potentials were measure and corrected accordingly. Mean current values represent the average of at least *n* oocytes (as indicated in each figure legend) and two or three donor frogs. Error bars denote SEM and are not shown when smaller than the symbol.

[^{14}C]-citrate efflux

Control, ZmMATE1- and ZmMATE2-expressing oocytes (2 days after cRNA injection) were injected with 23 nl of 460 μM [^{14}C]-citrate (1.15 nCi/oocyte). The cells (seven per replicate; $n = 4$) were allowed to recover for 3 min in ice-cold ND96 solution (pH 4.5), then transferred into 1.5 ml ND96 (pH 4.5) at room temperature. At the indicated time points, 0.75 ml of the bathing solution was removed and replaced with fresh buffer. At the end of each experiment, the cells were disrupted in scintillation fluid. Radioactivity from sampled efflux buffer at the various time points and remaining radioactivity in the oocytes was counted using full-spectrum disintegrations per minute counting in a Beckman Coulter LS6500 liquid scintillation counter (http://www.beckman.com).

Expression of *ZmMATE1* in transgenic Arabidopsis

The coding region (cDNA) of *ZmMATE1* was cloned into pBAR2 under the control of the 35S promoter. Both empty vector and the vector carrying the construct were transformed into Arabidopsis using *Agrobacterium tumefaciens* via the floral dip method (Clough and Bent, 1998). Transformants were selected by spraying T_1 seedlings with the herbicide ammonium glufosinate (Sigma-Aldrich, http://www.sigmaaldrich.com), and the presence of the transgene was confirmed via PCR of the T-DNA insertions. Transgenic plants were selfed and the progenies screened as above for two generations. Homozygous T_3 lines were identified via progeny testing of T_4 seeds. Al tolerance and root citrate release were analyzed in homozygous T_3 lines as follows. Al tolerance based on root growth was assayed in agar plates according to Ryan *et al.* (2007). In brief, seeds were surface-sterilized, stratified at 4°C for 3 days, then sown onto plates with sterile growth medium containing 0 or 500 μM $AlCl_3$ (pH 4.8). Approximately 60 seeds of each line including wild-type Columbia were placed in a straight line across the agar plates. Plates were then placed in a growth chamber at 20°C in a near-vertical position so that the line of seeds was horizontal. Roots were measured after 2 weeks. Root citrate release was measured as described by Hoekenga *et al.* (2006) with modifications. Approximately 200 sterilized stratified seeds were grown in hydroponic nutrient solution (pH 4.2) for 5 days, then the medium was replaced by the same medium containing 0 or 12.5 μM $AlCl_3$. After 24 h, plants were transferred to 25 ml of exudation medium (pH 4.2) with or without Al (12.5 μM $AlCl_3$); root exudates were collected after 24 h and analyzed by capillary electrophoresis. Prior to analysis, the samples were treated with a cation-exchange resin (Dowex 50wx8, H^+ form, 100:1 v/w, http://www.dow.com/liquidseps/) to remove Al. Organic acids were quantified using a Beckman MDQ capillary electrophoresis system (http://www.beckman.com). Anions were separated in a 67 cm capillary (75 μm internal diameter) with a constant voltage of −20 kV at 25°C. The background buffer consisted of 0.5 mM dodecyltrimethylammonium bromide, 7.5 mM salicylic acid and 15 mM Tris, pH 8.2. Peaks were resolved using a UV absorbance detector at 230 nm wavelength. Organic acids were identified on the basis of their migration time relative to standards, with subsequent confirmation by spiking samples with specific organic acids.

ACKNOWLEDGEMENTS

The authors would like to thank Eric Craft and Randy Clark for technical assistance during the development of this work. The work was supported by NSF Plant Genome Research Grant DBI number 0419435, Grant Generation Challenge Program grant number G3008.02, USDA National Research Initiative competitive grant number 2006-35301-16884, a McKnight Foundation Collaborative Crop Research Program grant, and a FAPEMIG–Brazil grant.

REFERENCES

Arai, M., Mitsuke, H., Ikeda, M., Xia, J.X., Kikuchi, T., Satake, M. and Shimizu, T. (2004) ConPred II: a consensus prediction method for obtaining transmembrane topology models with high reliability. *Nucleic Acids Res.* **32**, W390–W393.

Barcelo, J. and Poschenrieder, C. (2002) Fast root growth responses, root exudates, and internal detoxification as clues to the mechanisms of aluminium toxicity and resistance: a review. *Environ. Exp. Bot.* **48**, 75–92.

Borrero, J.C., Pandey, S., Ceballos, H., Magnavaca, R. and Bahia, A.F.C. (1995) Genetic variances for tolerance to soil acidity in a tropical maize population. *Maydica*, **40**, 283–288.

Bortiri, E., Jackson, D. and Hake, S. (2006) Advances in maize genomics: the emergence of positional cloning. *Curr. Opin. Plant Biol.* **9**, 164–171.

Brem, R.B., Yvert, G., Clinton, R. and Kruglyak, L. (2002) Genetic dissection of transcriptional regulation in budding yeast. *Science*, **296**, 752–755.

Clough, S.J. and Bent, A.F. (1998) Floral dip: a simplified method for *Agrobacterium*-mediated transformation of *Arabidopsis thaliana*. *Plant J.* **16**, 735–743.

Collins, N.C., Shirley, N.J., Saeed, M., Pallotta, M. and Gustafson, J.P. (2008) An *ALMT1* gene cluster controlling aluminum tolerance at the *Alt4* locus of rye (*Secale cereale* L.). *Genetics*, **179**, 669–682.

Debeaujon, I., Peeters, A.J.M., Leon- Kloosterziel, K.M. and Koornneef, M. (2001) The *TRANSPARENT TESTA12* gene of Arabidopsis encodes a multidrug secondary transporter-like protein required for flavonoid sequestration in vacuoles of the seed coat endothelium. *Plant Cell*, **13**, 853–871.

Durrett, T.P., Gassmann, W. and Rogers, E.E. (2007) The FRD3-mediated efflux of citrate into the root vasculature is necessary for efficient iron translocation. *Plant Physiol.* **144**, 197–205.

Furukawa, J., Yamaji, N., Wang, H., Mitani, N., Murata, Y., Sato, K., Katsuhara, M., Takeda, K. and Ma, J.F. (2007) An aluminum-activated citrate transporter in barley. *Plant Cell Physiol.* **48**, 1081–1091.

Goldin, A.L. (1992) Maintenance of *Xenopus laevis* and oocyte injection. *Methods Enzymol.* **207**, 266–279.

Henikoff, S. and Henikoff, J.G. (1992) Amino acid substitution matrices from protein blocks. *Proc. Natl. Acad. Sci. USA*, **89**, 10915–10919.

Hoekenga, O.A., Maron, L.G., Pineros, M.A. *et al.* (2006) *AtALMT1*, which encodes a malate transporter, is identified as one of several genes critical for aluminum tolerance in Arabidopsis. *Proc. Natl Acad. Sci. USA*, **103**, 9738–9743.

Huang, C.F., Yamaji, N., Mitani, N., Yano, M., Nagamura, Y. and Ma, J.F. (2009) A bacterial-type ABC transporter is involved in aluminum tolerance in rice. *Plant Cell*, **21**, 655–667.

Kao, C.H., Zeng, Z.B. and Teasdale, R.D. (1999) Multiple interval mapping for quantitative trait loci. *Genetics*, **152**, 1203–1216.

Kidd, P.S., Llugany, M., Poschenrieder, C., Gunse, B. and Barcelo, J. (2001) The role of root exudates in aluminium resistance and silicon-induced amelioration of aluminium toxicity in three varieties of maize (*Zea mays* L.). *J. Exp. Bot.* **52**, 1339–1352.

Kochian, L.V., Hoekenga, O.A. and Piñeros, M.A. (2004) How do crop plants tolerate acid soils? Mechanisms of aluminum tolerance and phosphorous efficiency. *Annu. Rev. Plant Biol.* **55**, 459–493.

Kosambi, D.D. (1944) The estimation of map distances from recombination values. *Ann. Eugenet.* **12**, 172–175.

Li, L.G., He, Z.Y., Pandey, G.K., Tsuchiya, T. and Luan, S. (2002) Functional cloning and characterization of a plant efflux carrier for multidrug and heavy metal detoxification. *J. Biol. Chem.* **277**, 5360–5368.

Ligaba, A., Katsuhara, M., Ryan, P.R., Shibasaka, M. and Matsumoto, H. (2006) The *BnALMT1* and *BnALMT2* genes from rape encode aluminum-activated malate transporters that enhance the aluminum resistance of plant cells. *Plant Physiol.* **142**, 1294–1303.

Liu, J.P., Magalhaes, J.V., Shaff, J. and Kochian, L.V. (2009) Aluminum-activated citrate and malate transporters from the MATE and ALMT families function independently to confer Arabidopsis aluminum tolerance. *Plant J.* **57**, 389–399.

Magalhaes, J.V., Garvin, D.F., Wang, Y.H., Sorrells, M.E., Klein, P.E., Schaffert, R.E., Li, L. and Kochian, L.V. (2004) Comparative mapping of a major aluminum tolerance gene in sorghum and other species in the Poaceae. *Genetics*, **167**, 1905–1914.

Magalhaes, J.V., Liu, J., Guimaraes, C.T. *et al.* (2007) A gene in the multidrug and toxic compound extrusion (MATE) family confers aluminum tolerance in sorghum. *Nat. Genet.* **39**, 1156–1161.

Magnavaca, R., Gardner, C. and Clark, R. (1987) Evaluation of inbred maize lines for aluminum tolerance in nutrient solution. In *Genetic Aspects of Plant Mineral Nutrition* (Gabelman, H.L.B., ed). Dordrecht, The Netherlands: Martinus Nijhoff, pp. 255–265.

Maron, L.G., Kirst, M., Mao, C., Milner, M.J., Menossi, M. and Kochian, L.V. (2008) Transcriptional profiling of aluminum toxicity and tolerance responses in maize roots. *New Phytol.* **179**, 116–128.

Morita, M., Shitan, N., Sawada, K., Van Montagu, M.C.E., Inzé, D., Rischer, H., Goossens, A., Oksman-Caldentey, K.M., Moriyama, Y. and Yazaki, K. (2009) Vacuolar transport of nicotine is mediated by a multidrug and toxic compound extrusion (MATE) transporter in *Nicotiana tabacum*. *Proc. Natl Acad. Sci. USA*, **106**, 2447–2452.

Moriyama, Y., Hiasa, M., Matsumoto, T. and Omote, H. (2008) Multidrug and toxic compound extrusion (MATE)-type proteins as anchor transporters for the excretion of metabolic waste products and xenobiotics. *Xenobiotica*, **38**, 1107–1118.

Ninamango- Cárdenas, F.E., Guimaraes, C.T., Martins, P.R., Parentoni, S.N., Carneiro, N.P., Lopes, M.A., Moro, J.R. and Paiva, E. (2003) Mapping QTLs for aluminum tolerance in maize. *Euphytica*, **130**, 223–232.

Omote, H., Hiasa, M., Matsumoto, T., Otsuka, M. and Moriyama, Y. (2006) The MATE proteins as fundamental transporters of metabolic and xenobiotic organic cations. *Trends Pharmacol. Sci.* **27**, 587–593.

Otani, M., Shitan, N., Sakai, K., Martinoia, E., Sato, F. and Yazaki, K. (2005) Characterization of vacuolar transport of the endogenous alkaloid berberine in *Coptis japonica*. *Plant Physiol.* **138**, 1939–1946.

Pandey, S., Ceballos, H., Magnavaca, R., Bahia, A.F.C., Duquevargas, J. and Vinasco, L.E. (1994) Genetics of tolerance to soil acidity in tropical maize. *Crop Sci.* **34**, 1511–1514.

Parker, D., Norvell, W.A. and Chaney, R.L. (1995) GEOCHEM-PC: a chemical speciation program for IBM and compatible personal computers. In *Chemical Equilibrium Reaction Models* (Leoppert, R., Schwab, A. and Goldberg, S., eds). Madison, WI: Soil Science Society of America, pp. 253–269.

Pellet, D.M., Grunes, D.L. and Kochian, L.V. (1995) Organic-acid exudation as an aluminum-tolerance mechanism in maize (*Zea mays* L). *Planta*, **196**, 788–795.

Piñeros, M.A., Magalhaes, J.V., Carvalho Alves, V.M. and Kochian, L.V. (2002) The physiology and biophysics of an aluminum tolerance mechanism based on root citrate exudation in maize. *Plant Physiol.* **129**, 1194–1206.

Piñeros, M.A., Shaff, J.E., Manslank, H.S., Alves, V.M.C. and Kochian, L.V. (2005) Aluminum resistance in maize cannot be solely explained by root organic acid exudation. A comparative physiological study. *Plant Physiol.* **137**, 231–241.

Piñeros, M.A., Cancado, G.M.A. and Kochian, L.V. (2008) Novel properties of the wheat aluminum tolerance organic acid transporter (TaALMT1) revealed by electrophysiological characterization in Xenopus oocytes: functional and structural implications. *Plant Physiol.* **147**, 2131–2146.

Raman, H., Zhang, K.R., Cakir, M. *et al.* (2005) Molecular characterization and mapping of *ALMT1*, the aluminium-tolerance gene of bread wheat (*Triticum aestivum* L.). *Genome*, **48**, 781–791.

Riede, C.R. and Anderson, J.A. (1996) Linkage of RFLP markers to an aluminum tolerance gene in wheat. *Crop Sci.* **36**, 905–909.

Ryan, P.R., Liu, Q., Sperling, P., Dong, B., Franke, S. and Delhaize, E. (2007) A higher plant Δ8 sphingolipid desaturase with a preference for (*Z*)-isomer formation confers aluminum tolerance to yeast and plants. *Plant Physiol.* **144**, 1968–1977.

Ryan, P.R., Raman, H., Gupta, S., Horst, W.J. and Delhaize, E. (2009) A second mechanism for aluminum resistance in wheat relies on the constitutive efflux of citrate from roots. *Plant Physiol.* **149**, 340–351.

Sasaki, T., Yamamoto, Y., Ezaki, B., Katsuhara, M., Ahn, S.J., Ryan, P.R., Delhaize, E. and Matsumoto, H. (2004) A wheat gene encoding an aluminum-activated malate transporter. *Plant J.* **37**, 645–653.

Sawaki, Y., Iuchi, S., Kobayashi, Y. *et al.* (2009) STOP1 regulates multiple genes that protect Arabidopsis from proton and aluminum toxicities. *Plant Physiol.* **150**, 281–294.

Sibov, S.T., Gaspar, M., Silva, M.J., Ottoboni, L.M.M., Arruda, P. and Souza, A.P. (1999) Two genes control aluminum tolerance in maize: genetic and molecular mapping analyses. *Genome*, **42**, 475–482.

Tzfira, T., Tian, G.W., Lacroix, B., Vyas, S., Li, J.X., Leitner-Dagan, Y., Krichevsky, A., Taylor, T., Vainstein, A. and Citovsky, V. (2005) pSAT vectors: a modular series of plasmids for autofluorescent protein tagging and expression of multiple genes in plants. *Plant Mol. Biol.* **57**, 503–516.

Uhde-Stone, C., Zinn, K.E., Ramirez-Yanez, M., Li, A.G., Vance, C.P. and Allan, D.L. (2003) Nylon filter arrays reveal differential gene expression in proteoid roots of white lupin in response to phosphorus deficiency. *Plant Physiol.* **131**, 1064–1079.

West, M.A.L., Kim, K., Kliebenstein, D.J., van Leeuwen, H., Michelmore, R.W., Doerge, R.W. and Clair, D.A.S. (2007) Global eQTL mapping reveals the complex genetic architecture of transcript-level variation in Arabidopsis. *Genetics*, **175**, 1441–1450.

Yokosho, K., Yamaji, N., Ueno, D., Mitani, N. and Ma, J.F. (2009) OsFRDL1 is a citrate transporter required for efficient translocation of iron in rice. *Plant Physiol.* **149**, 297–305.

Yoo, S.D., Cho, Y.H. and Sheen, J. (2007) Arabidopsis mesophyll protoplasts: a versatile cell system for transient gene expression analysis. *Nat. Protoc.* **2**, 1565–1572.

The Genbank accession numbers for the sequences A–F are FJ015155, FJ015156, FJ015157, FJ873684, FJ873685 and FJ873686, respectively.

